# QCD predictions for deep-inelastic structure functions at the DESY *ep* collider HERA

A. J. Askew, J. Kwiecinski,* A. D. Martin, and P. J. Sutton
*Department of Physics, University of Durham, DH1 3LE, England*
(Received 10 December 1992)

Perturbative QCD is used to predict the deep-inelastic electron-proton structure functions $F_{T,L}(x,Q^2)$ in the small $x$ region ($x \sim 10^{-3}$) from an experimental knowledge of the behavior at larger $x$. Shadowing corrections are quantified.

PACS number(s): 13.60.Hb, 12.38.Bx

## I. INTRODUCTION

The DESY *ep* collider HERA is poised to measure the structure functions $F_i(x,Q^2)$ for deep-inelastic electron-proton scattering in the small $x$ region, typically $x \sim 10^{-3}$ and $Q^2 \sim 10$ GeV$^2$ [1]; a region so far unprobed by experiment but in which novel effects are expected to occur. Perturbative QCD predicts, via a leading $\ln(1/x)$ summation of multiple soft gluon emissions, that the structure functions will have a singular $x^{-\lambda}$ behavior at small $x$, with $\lambda$ possibly as large as 0.5. The summation is carried out by the Lipatov equation [2] and the resulting behavior is therefore said to arise from the "Lipatov" (or bare QCD) Pomeron, which has intercept $\alpha_P = 1+\lambda$ considerably above unity. Ultimately, with decreasing $x$, the singular behavior must be suppressed by shadowing corrections, and eventually by nonperturbative effects.

So far the only way to explore these novel effects has been to extrapolate parton distributions from the region $x > 0.01$ where they are determined by existing deep-inelastic data into the small $x$ region. Although such extrapolations are notoriously unreliable, they do provide useful information on the general trend. Figure 1 shows the $x$ behavior of $F_2(x,Q^2)$ as obtained in the most recent global structure function analysis [3]. It shows extrapolations based on two sets of partons, $D_-$ and $D_0$, which respectively include and omit an $x^{-\frac{1}{2}}$ factor designed to mock up the Lipatov small $x$ behavior. Both sets describe the whole range of existing precise deep-inelastic data equally well. We see that it will be difficult to experimentally distinguish the need for an $x^{-\frac{1}{2}}$ factor from the forthcoming measurements of $F_2(x,Q^2)$ in the region $x \sim 10^{-3}$. The dashed curve in Fig. 1, obtained from parton distributions which contain shadowing corrections, shows that the screening effects are expected to be small in this $x$ region. We emphasize that the small $x$ predictions shown in Fig. 1 are simply extrapolations of parametric forms determined from data which, apart from one or two measurements, populate the $x \gtrsim 0.05$ region. A missing ingredient is any constraint on the size of the Lipatov component. The gluon distribution has not been required to satisfy the Lipatov equation at small $x$; simply, a leading $x^{-\frac{1}{2}}$ behavior has been imposed on the "starting" distribution at some $Q^2 = Q_0^2$, and also on the sea quark distributions which are themselves driven by the gluon. We should add, though, that it was subsequently shown that the form of the gluon was quite compatible with that obtained by numerical solution of the Lipatov equation [4].

Here we present more quantitative predictions of the behavior of $F_2(x,Q^2)$, and the longitudinal structure function $F_L(x,Q^2)$, at small $x$. Since the density of gluons increases rapidly with decreasing $x$ the sea quark distributions are increasingly dominated by the gluon distribution, via $g \to q\bar{q}$. This component may be calculated in perturbative QCD. The relevant diagram is shown in Fig. 2. The contribution to the (transverse and longitudinal) deep-inelastic structure functions may therefore

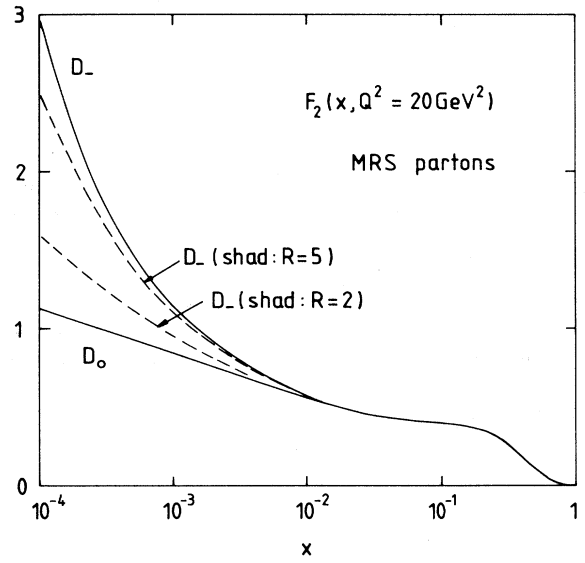


FIG. 1. Extrapolations of $F_2$ at $Q^2 = 20$ GeV$^2$ to small $x$ based on MRS partons [3]. Sets $D_-$ and $D_0$ have $xg, xq_{\rm sea}$ "starting" distributions (that is at $Q_0^2 = 4$ GeV$^2$) which behave respectively as $x^{-\frac{1}{2}}$ and $x^0$ at small $x$. The dashed curves show the effect of conventional parton shadowing with $R = 5$ GeV$^{-1}$ together with the more extreme "hot spot" shadowing with $R = 2$ GeV$^{-1}$.

*On leave from the H. Niewodniczanski Institute of Nuclear Physics, 31-342 Krakow, Poland.

 

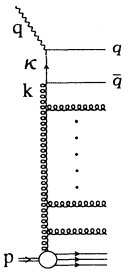


FIG. 2. Diagrammatic representation of a gluon "ladder" contribution to the deep-inelastic structure functions of the proton. $q, \kappa, k$, and $p$ denote the particle four-momenta.

be written in the factorizable form [5–7]

$$F_{T,L}(x,Q^2) = \int_x^1 \frac{dx'}{x'} \int \frac{dk_T^2}{k_T^4} f\left(\frac{x}{x'}, k_T^2\right) F_{T,L}^{(0)}(x', k_T^2, Q^2), \quad (1)$$

see Fig. 3, where $x/x'$ is the longitudinal momentum fraction carried by the gluon which dissociates into the $q\bar{q}$ pair. The function $F^{(0)}$ denotes the quark box (and crossed box) approximation to the photon-gluon subprocess shown in the upper part of Fig. 3. In other words, $F^{(0)}$, or rather to be dimensionally correct $F^{(0)}/k_T^2$, may be regarded as the structure function of a gluon of approximate virtuality $k_T^2$. The gluon density function $f$ in (1) denotes the sum of the ladder diagrams shown in the lower part of Fig. 3. In the leading $\ln(1/x)$ approximation, $f$ is given as the solution of the Lipatov equation; for this reason it is the "unintegrated" gluon density

$$f(x,k_T^2) = \left.\frac{\partial(xg(x,Q^2))}{\partial \ln Q^2}\right|_{Q^2=k_T^2}. \quad (2)$$

The function $g(x,Q^2)$, which enters (2), is the traditional gluon distribution whose $Q^2$ evolution is controlled by the Altarelli-Parisi equations and whose form is determined by the parton analyses of the deep-inelastic structure function data. It is therefore instructive to see how the general factorizable form (1) reduces to the Altarelli-Parisi evolution of $q\bar{q}$ radiation from a gluon. In the Altarelli-Parisi treatment in the leading $\ln Q^2$ approximation the integrations over the transverse momenta are

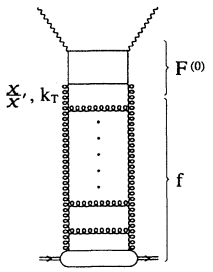


FIG. 3. Diagrammatic representation of the factorization formula of Eq. (1).

dominated by the contributions from the strongly ordered configuration $k_T^2 \ll \kappa_T^2 \ll Q^2$, where the momenta $k, \kappa$, and $q$ are shown in Fig. 3 and where $Q^2 \equiv -q^2$. In this limit there is no contribution to $F_L$ and so we need only consider $F_2(x,Q^2)$. If we keep only the strongly ordered contribution and we recall that $x'$ is the momentum fraction of the gluon carried by the quark (or antiquark) which is struck by the photon, then $F^{(0)}$ of (1) is given by

$$F_2^{(0)}(x', k_T^2, Q^2)/k_T^2 = \int_{k_T^2}^{Q^2} \frac{d\kappa_T^2}{\kappa_T^2} 2 \sum_q e_q^2 \frac{\alpha_s(\kappa_T^2)}{2\pi} x' P_{qg}(x'), \quad (3)$$

where $P_{qg}$ is the Altarelli-Parisi splitting function. Thus (1) becomes

$$F_2(x,Q^2) = \int_x^1 dx' \int^{Q^2} \frac{d\kappa_T^2}{\kappa_T^2} \int^{\kappa_T^2} \frac{dk_T^2}{k_T^2} f\left(\frac{x}{x'}, k_T^2\right) \times 2 \sum_q e_q^2 \frac{\alpha_s(\kappa_T^2)}{2\pi} P_{qg}(x') \quad (4)$$

and hence, using (2), we have

$$\frac{\partial F_2}{\partial \ln Q^2} = 2 \sum_q e_q^2 \frac{\alpha_s(Q^2)}{2\pi} \int_x^1 dx' P_{qg}(x') \frac{x}{x'} g\left(\frac{x}{x'}, Q^2\right), \quad (5)$$

that is the conventional Altarelli-Parisi evolution of $F_2$ driven by $g \to q\bar{q}$.

There are at least two reasons why the leading $\ln Q^2$ evolution (5) is inadequate in the small $x$ region. The first is due to the Lipatov effect and the second arises from shadowing. We discuss these effects in turn. A crucial observation is that it is the dominance of the region of strong ordering of the transverse momenta which leads to the nested logarithmic integrations of (4). However at small $x$ where the leading $\ln(1/x)$ terms dominate it is important to retain the full $Q^2$ dependence and not just the leading $\ln Q^2$ terms. This is accomplished by the Lipatov equation for the unintegrated distribution $f$ which sums the ladder diagrams over the full phase space of the transverse momenta and not simply the strongly ordered part. In the case of fixed $\alpha_s$ the Lipatov equation may be approximately solved analytically. The leading small $x$ behavior is found to be

$$f(x,k_T^2) \propto (k_T^2)^{\frac{1}{2}} \frac{x^{-\lambda}}{\sqrt{\ln(1/x)}} \left[1 + O\left(\frac{1}{\ln(1/x)}\right)\right], \quad (6)$$

where

$$\lambda = \frac{3\alpha_s}{\pi} 4 \ln 2. \quad (7)$$

We note, in particular, the factor $(k^2)^{\frac{1}{2}}$ which may be traced to the anomalous dimension having magnitude $\frac{1}{2}$ [2, 5]. Because of this factor, the region of strongly ordered transverse momenta is no longer dominant. The integrals are no longer of logarithmic $dk_T^2/k_T^2$ form and

we must use the exact $k_T^2$ dependence of $F^{(0)}$ as well as integrating over the full region of phase space of the transverse momenta. This has been found to have profound effects on the predictions for heavy-quark photo- and electro-production [5]. (The cross sections can increase by a factor of 3 when the effects of shifted anomalous dimension are included.)

As $x$ decreases, the singular $x^{-\lambda}$ behavior of $f$ will eventually be tamed by shadowing effects. These stop $f$ from growing with decreasing $x$ and lead to an $x$-independent saturation limit which grows linearly with $k_T^2$ [8], that is,

$$f_{\rm sat}(x,k_T^2) \sim R^2 k_T^2, \tag{8}$$

where the radius $R$ specifies the (transverse) region in which the gluons are concentrated within the proton. As before, the $k_T^2$ behavior requires that we must integrate over the full domain of the transverse momenta.

The above two formulas (6) and (8) overestimate their respective effects. The numerical solution of the Lipatov equation shows, particularly when the effects of the running of $\alpha_s$ are included, that the approximate analytic form (6) considerably overestimates the actual solution [9]. Secondly, the numerical solution of the Lipatov equation with the nonlinear shadowing contribution included shows that the saturation limit (8) is approached rather slowly and that it is irrelevant for the $x \gtrsim 10^{-4}$ region which will be probed at HERA [4]. In particular, we are able to obtain more definitive estimates of the size of the shadowing corrections than hitherto.

We have concentrated on using the Lipatov equation in an attempt to make absolute predictions of $F_{T,L}(x,Q^2)$ in the small $x$ region from perturbative QCD. As mentioned above, the Lipatov equation yields $f(x,k_T^2)$ by summing the leading $\ln(1/x)$ terms, whilst retaining the full $k_T^2$ dependence (rather than just the leading $\ln k_T^2$ contributions). However to ensure a reliable prediction for the $k_T^2$ dependence we should really be even-handed and also include leading $\ln k_T^2$ terms which are nonleading in $\ln(1/x)$. These contributions, which are beyond the scope of this work, are discussed further in Sec. IV.

It is illuminating to consider the full content of the factorization formula (1) for $F_{T,L}(x,Q^2)$. The formula, with the exact functions $F_{T,L}^{(0)}$ arising from the quark box and crossed box diagrams, does not describe just photon-gluon interactions in which the exchanged quark and gluon are constituents of the proton. For sufficiently small $Q^2$, the formula also describes the situation in which the exchanged quark is better regarded as a constituent of the photon; that is when the quark lies in the photon (rather than the proton) hemisphere and when $k_T^2 \gg \kappa_T^2 \gtrsim Q^2$, where the momenta are defined in Fig. 2. These kinematic conditions could also apply to the gluon and then Fig. 2 would describe a semi-hard interaction between this gluon constituent of the photon and a gluon constituent of the proton (the next gluon down the chain with $k_T'^2 \gg k_T^2 \gtrsim Q^2$). Since we shall integrate over the full momentum phase space of the outgoing particles in Fig. 2 all these contributions are automatically included. In practice, the gluon emissions are subjected to a kinematic cutoff ($k_T^2 > k_0^2$) and so part of the nonperturbative gluon content of the photon will be excluded. Also formula (1) does not, of course, include the vector-meson-dominance component of the photon.

The primary purpose of this paper is to use (1) to estimate the deep-inelastic structure functions $F_2$ and $F_L$ at small $x$ using the exact solution $f$ of the Lipatov equation (with and without the shadowing term) and using the exact forms of the photon-gluon couplings $F_{T,L}^{(0)}$. In this way we are able to make "absolute" predictions for the contribution to $F_2$ and $F_L$, in the small $x$ region, arising from the leading $\ln(1/x)$ gluon summation, which in turn drives the sea quark contributions via $g \to q\bar{q}$. We calculate the remaining ("background") contribution to $F_2$ using phenomenologically known structure functions (and parton distributions) at larger $x$. The background contributions to $F_2$ and $F_L$ turn out to be approximately independent of $x$ in the small $x$ region, and to be small for $F_L$. The "absolute" predictions, however, are subject to several ambiguities: the choice of the infrared cutoff, the size of the shadowing radius parameter $R$, etc. We quantify these uncertainties in Sec. III.

It is worth mentioning that there are dynamical calculations of parton distributions [10] in which the sea quark and gluon distributions at large scales are obtained by evolving with Altarelli-Parisi equations from "valence" quark (and "valence" gluon) distributions at some (very) low $Q^2$ scale. A similar attempt to calculate the gluon and sea quark distributions entirely within perturbative QCD is presented in Ref. [11]. These calculations are ambitious and speculative in that they stretch the application of perturbative QCD to very low scales, but since they do not take into account the Lipatov leading $\ln(1/x)$ terms implied by perturbative QCD they do not generate the complete small $x$ behavior of $F_2$ and $F_L$. The validity of using perturbative QCD to dynamically generate parton distributions from valencelike input at low $Q^2$ has recently been questioned [12].

## II. SMALL $x$ BEHAVIOR OF $F_T$ AND $F_L$ FROM PERTURBATIVE QCD

We use the factorization formula (1) to evaluate the small $x$ behavior of the deep-inelastic structure functions

$$F_T = 2xF_1, \tag{9}$$

$$F_L = F_2 - 2xF_1. \tag{10}$$

The relevant diagrams are shown in Fig. 4, where the uppermost gluon in the ladder couples to the virtual photon through the quark box and "crossed box" diagrams respectively.

Concentrating on the box diagrams it is convenient to use the basic lightlike momenta $q'$ and $p$ where

$$q' = q + xp,$$

where, as usual, $x = Q^2/2p\cdot q$ and $Q^2 = -q^2$. We decompose the gluon and quark four-momenta, $k$ and $\kappa$

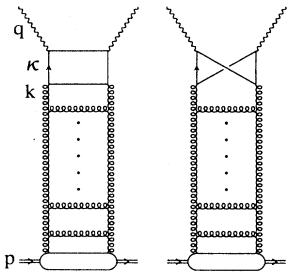


FIG. 4. Diagrams giving the small $x$ behavior of the structure functions for deep-inelastic electron-proton scattering.

respectively, in terms of the Sudakov variables

$$k = ap - bq' + k_T, \qquad \kappa = \alpha p - \beta q' + \kappa_T. \tag{11}$$

We must carry out the integration over the box diagrams subject to quark mass-shell constraints which, in terms of the Sudakov variables, are of the form

$$(\alpha - x)2p\cdot q(1-\beta) - \kappa_T^2 = m^2, \tag{12}$$

$$(a-\alpha)2p\cdot q\beta - (\boldsymbol{\kappa}_T - \boldsymbol{k}_T)^2 = m^2. \tag{13}$$

For the charm quark, $m$ is taken to be $m_c = 1.7$ GeV, whereas the light $u$, $d$, and $s$ quarks are taken to be massless. The first condition, Eq. (12), fixes $\alpha$. If we eliminate $\alpha$ from (13), we obtain

$$(a-x)\beta(1-\beta)2p\cdot q - \beta\kappa_T^2 - (1-\beta)(\boldsymbol{\kappa}_T - \boldsymbol{k}_T)^2 = m^2. \tag{14}$$

Next we remove the dependence on the azimuthal angle by changing the variable $\kappa_T$ to [5, 6]

$$\kappa'_T = \kappa_T - (1-\beta)k_T. \tag{15}$$

Then (14) becomes

$$(a-x)\beta(1-\beta)2p\cdot q - \beta(1-\beta)k_T^2 - \kappa_T'^2 = m^2. \tag{16}$$

This will allow the azimuthal integration to be performed analytically.

We are now ready to evaluate (1), and in particular the box contributions, $F^{(0)}$. We may express the contributions of the diagrams of Fig. 4 in the form [6, 13, 14]

$$F_T(x,Q^2) = 2\sum_q e_q^2 \frac{Q^2}{4\pi^2}\int_{k_0^2}\frac{dk_T^2}{k_T^4}\int_0^1 d\beta \int d^2\kappa'_T\,\alpha_s(\kappa_T'^2 + m_0^2) \times \left\{[\beta^2 + (1-\beta)^2]\left[\frac{\kappa_T^2}{D_1^2} - \frac{\boldsymbol{\kappa}_T\cdot(\boldsymbol{\kappa}_T - \boldsymbol{k}_T)}{D_1 D_2}\right] + \frac{m^2}{D_1^2} - \frac{m^2}{D_1 D_2}\right\} f\left(\frac{x}{x'}, k_T^2\right), \tag{17}$$

$$F_L(x,Q^2) = 2\sum_q e_q^2 \frac{Q^4}{\pi^2}\int_{k_0^2}\frac{dk_T^2}{k_T^4}\int_0^1 d\beta\,\beta^2(1-\beta)^2 \int d^2\kappa'_T\,\alpha_s(\kappa_T'^2 + m_0^2)\left[\frac{1}{D_1^2} - \frac{1}{D_1 D_2}\right] f\left(\frac{x}{x'}, k_T^2\right), \tag{18}$$

where

$$D_1 = \kappa_T^2 + \beta(1-\beta)Q^2 + m^2,$$

$$D_2 = (\boldsymbol{\kappa}_T - \boldsymbol{k}_T)^2 + \beta(1-\beta)Q^2 + m^2, \tag{19}$$

with $\kappa_T = \kappa'_T + (1-\beta)k_T$ in (17)–(19), see (15). The $x'$ integration of (1) is implicit in the $d^2\kappa'_T$ and $d\beta$ integrations. Indeed $x'$ is fixed in terms of $\kappa'_T$ and $\beta$ by (16). If we note that $a = x/x'$ then (16) gives

$$x' = \left[1 + \frac{\kappa_T'^2 + m^2}{Q^2}\beta(1-\beta) + \frac{k_T^2}{Q^2}\right]^{-1}.$$

The requirement that $0 < x' < 1$ is clearly satisfied. Of course the integration regions of (17) and (18) must be additionally constrained by the condition

$$x'(\beta, \kappa_T'^2, k_T^2, Q^2) > x \tag{20}$$

so that the argument $z = x/x'$ of $f$ satisfies the requirement $z < 1$. The argument of $\alpha_s$ has been taken to be $\kappa_T'^2 + m_0^2$ in (17) and (18), which allows integration over the entire region of $\kappa'_T$, since for small $\kappa_T'^2$ the "mass" $m_0$ serves as the regulator by "freezing" the coupling to $\alpha_s(m_0^2)$. For the light quarks we take $m_0^2 = 1$ GeV$^2$; the results are not very sensitive to variations of $m_0$ about this value. For the charm quark contribution we set $m_0^2 = m_c^2$. One final point to note is that the choice of argument of $\alpha_s$ has the advantage that in the strongly ordered configuration with large $Q^2$ we have $\alpha_s(\kappa_T^2)$, while for $k_T^2 \gg \kappa_T^2$ we have essentially $\alpha_s(k_T^2)$.

Expressions (17) and (18) for the deep-inelastic structure functions are the explicit realization of the factorization formula (1). Therefore, provided the gluon distribution $f(z, k_T^2)$ is known, we can calculate $F_T$ and $F_L$. For small $z$ the function $f(z, k_T^2)$ is calculated in the leading $\ln(1/z)$ approximation from the Lipatov equation, which may be written in the integro-differential form

$$z\frac{\partial f(z,k_T^2)}{\partial z} = \frac{3\alpha_s(k_T^2)}{\pi}k_T^2\int_{k_0^2}^{\infty}\frac{dk_T'^2}{k_T'^2}\left\{\frac{f(z,k_T'^2) - f(z,k_T^2)}{|k_T'^2 - k_T^2|} + \frac{f(z,k_T^2)}{(4k_T'^4 + k_T^4)^{\frac{1}{2}}}\right\} \equiv K\otimes f. \tag{21}$$

If we incorporate the effects of parton shadowing the equation becomes [8, 4]

$$z\frac{\partial f(z,k_T^2)}{\partial z} = K\otimes f - \frac{81}{16k_T^2R^2}\alpha_s^2(k_T^2)[zg(z,k_T^2)]^2, \tag{22}$$

where

$$zg(z,k_T^2) = \int_{\tilde{k}_0^2}^{k_T^2}\frac{dk_T'^2}{k_T'^2}f(z,k'^2), \tag{23}$$

with $\tilde{k}_0^2 = 1$ GeV$^2$ [4]. Equation (23) is the inverse (2). The additional term, quadratic in $g$, in (22) is the leading-order shadowing contribution, the negative sign leading to a suppression in the growth of the gluon density with decreasing $z$, which arises from the recombination of gluons. It is the iteration of (22) that generates the "fan" diagrams in which the lines correspond to the Lipatov ladders [8]. For investigations of shadowing, the crucial parameter is $R$, which specifies the size of the region in which the gluons are concentrated within the proton.

Finally we mention a possible simplifying assumption that could be considered for the factorization formula (1). To leading $\ln(1/x)$ accuracy we may ignore the $x'$ dependence of $f(x/x',k_T^2)$ in (1). This is justified since

$$\left(\ln\frac{x}{x'}\right)^n = (\ln x)^n[1+O(1/\ln x)].$$

The technical advantage of using this approximation is that the constraint (20), which requires $x/x' < 1$, does not have to be imposed on the region of integration. For example, in a recent calculation by Levin and Ryskin [15], which motivated the present study, the saturation limit (8) was used for $f$ (at least for low $Q^2$). In such a case $f$ would be independent of $x$ and the simplifying approximation is reasonable. In general the simplifying approximation $f(x/x',k_T^2)\to f(x,k_T^2)$ is expected to overestimate the magnitude, but to lead to a satisfactory prediction for the shape of the small $x$ behavior of $F_T$ and $F_L$. For instance, if $f(z,k_T^2)\sim z^{-\lambda}$ then the approximation would amount to the omission of a factor $x'^{\lambda}$ in the implicit $x'$ integration.

## III. NUMERICAL QCD PREDICTIONS FOR $F_2$ AND $F_L$

We calculate the leading $\ln(1/x)$ contributions to $F_2 = F_T + F_L$ and $F_L$ using Eqs. (17) and (18). We first solve the integro-differential Lipatov equation (22) for $f(z,k_T^2)$ by evolving down in $z$ from boundary conditions at $z = z_0 = 10^{-2}$ specified in terms of the known gluon distribution $g(z_0,Q^2)$. The procedure is described in detail in Ref. [4]. Above $z_0$, where the Lipatov effect is expected to be negligible, we simply use the known gluon distribution to calculate $f(z,k_T^2)$ via (2). The "known" parton distributions that we use for $z\geq z_0$ are those of set $D_0$ of Ref. [3]; to be precise, we use $D_0$-type distributions which have been obtained by a global leading-order fit [16] to the deep-inelastic data, rather than those obtained in the next-to-leading-order analysis of Ref. [3].

In summary, the gluon distribution $f(x,k_T^2)$, or $g(x,Q^2)$, is determined from the Lipatov equation for $x < x_0$, and from deep-inelastic data via the Altarelli-Parisi evolution equations for $x\geq x_0$. Though the continuity of $g$ at $x = x_0$ is assured, there can be a mismatch of the derivatives on account of the different rates of $Q^2$ evolution in the two regions (see ref. [4]). We take up the discussion of this point in Sec. IV. However, it turns out, fortuitously, that the smoothest matching across the $x = x_0$ boundary occurs for $Q^2\simeq 10$–$20$ GeV$^2$ [4], the $Q^2$ region most pertinent to investigate the small $x$ behavior at HERA.

We show results for the structure functions $F_{2,L}$ at $Q^2 = 10$ and 20 GeV$^2$ corresponding to two choices ($k_0^2 = 1$ and 2 GeV$^2$) of the lower cutoff of the integration over the transverse momentum $k_T$ of the gluon in the Lipatov equation (21) and in the convolution formulas (17) and (18). Also, we present results with the shadowing term (quadratic in $g$) omitted from (22), and with it included for two different choices of $R$, where $\pi R^2$ is the transverse area within which the gluons are concentrated in the proton. We chose either $R = 5$ GeV$^{-1}$ (corresponding to gluons uniformly spread across the proton) or $R = 2$ GeV$^{-1}$ (gluons concentrated in "hot spots" within the proton). We then calculated $F_2$ and $F_L$ from (17) and (18) using the different solutions that we obtained for $f(z,k_T^2)$.

Before we present the above QCD predictions for $F_2$ and $F_L$ we must note that they are not the only contributions to the structure functions. They simply represent the leading $\ln(1/x)$ gluon contributions, which we denote $F_2^g$ and $F_L^g$. These contributions are indeed expected to dominate at small $x$, but they decrease rapidly with increasing $x$. The remaining contributions to the structure functions (which we denote $F_2^{\rm rem}$ and $F_L^{\rm rem}$) are calculated from the Altarelli-Parisi equations with the $1/z$ term omitted from the splitting function $P_{gg}(z)$. Again we use the "$D_0$" set of parton distributions [3, 16]. The results at $Q^2 = 10$ and 20 GeV$^2$ are shown in Figs. 5 and 6 respectively. The background contributions $F_2^{\rm rem}$ and $F_L^{\rm rem}$ are shown by the dot-dashed curves.

The agreement between the curves and the available data for $F_2$ shows that our input distributions for $x > x_0 = 0.01$ are satisfactory. The main purpose of this work is to use this "experimental" input to make theoretical extrapolations of $F_2(x,Q^2)$ and $F_L(x,Q^2)$ into the small $x$ region based on perturbative QCD. The results are shown by the continuous curves in Figs. 5 and 6 if shadowing is neglected, and by dashed curves if shadowing effects are included. Two examples of shadowing are shown: conventional shadowing corresponding to gluons uniformly distributed through the entire proton ($R = 5$ GeV$^{-1}$) and a more extreme scenario in which they are concentrated in "hot spots" ($R = 2$ GeV$^{-1}$) within the proton. Recall that the shadowing term in (22) is proportional to $1/R^2$.

We may compare the results of Figs. 5 and 6 with extrapolations based on sets of partons obtained from global analyses of deep-inelastic data {see, for example, Martin, Roberts, and Stirling (MRS) [3]}. We see that the unshadowed predictions are similar to the paramet-

ric extrapolation based on the $D_-$ set of partons [3], see Fig. 1. Recall that for the $D_-$ set an $x^{-\frac{1}{2}}$ factor was specially incorporated into the gluon and sea quark "starting" distributions [$xg(x,Q_0^2)$ and $x\overline{q}(x,Q_0^2)$] to mock up the shape due to the Lipatov effect. The magnitude of the Lipatov effect in $F_2$ obtained from the $D_-$ set is simply the result of extrapolation of a phenomenologically determined parametric form to small $x$; in contrast, in this work we solve the Lipatov equation in the small $x$ region with phenomenologically determined boundary conditions at $x = x_0$. From Figs. 5 and 6 we see that our predictions of the shadowing corrections are significantly smaller than those obtained in MRS [3] [or Kwiecinski-MRS (KMRS) [19]]. The present calculation has the advantage that it does not depend on assumed input parametric forms at $Q^2 = Q_0^2$ in the small $x$ region. Rather, our extrapolation is based on the known phenomenological behavior for $x > x_0$ and follows directly from solving the Lipatov equation with shadowing terms incorporated. In this sense it may be regarded as an "absolute" prediction.

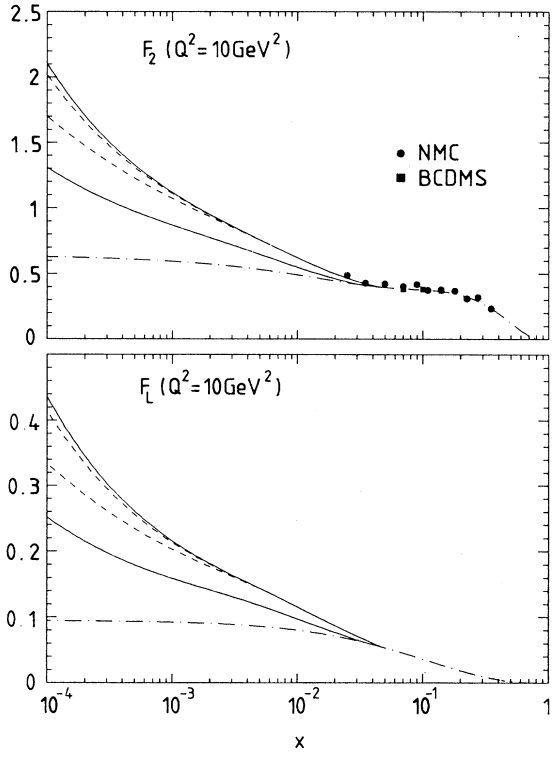


FIG. 5. Perturbative QCD predictions of the behavior of the structure functions $F_2(x,Q^2)$ and $F_L(x,Q^2)$ at $Q^2 = 10$ GeV$^2$ and small $x$. The continuous curves are with shadowing neglected, while the upper (lower) dashed curves have shadowing effects included with $R = 5$ GeV$^{-1}$ ($R = 2$ GeV$^{-1}$). For the upper three curves the infrared cutoff in (21) is chosen to be $k_0^2 = 1$ GeV$^2$, while the lowest continuous curves give the unshadowed result for $k_0^2 = 2$ GeV$^2$. The dot-dashed curves are the background (non-Lipatov) contributions. The data are from the New Muon Collaboration (NMC) [17] and the BCDMS collaboration [18].

The origin of the larger shadowing corrections found in the MRS [3] (and KMRS [19]) structure function analyses can be traced to the assumption that the sea quark "starting" distributions in the region $x < x_0$ are taken to have shadowing corrections proportional to those of the gluon, that is

$$\overline{q}_{\rm shad}(x,Q_0^2) = \overline{q}_{\rm unshad}(x,Q_0^2)\frac{g_{\rm shad}(x,Q_0^2)}{g_{\rm unshad}(x,Q_0^2)},$$

see Eq. (35) of Ref. [19]. It could be argued that a more reliable estimate would have been to take the argument of $x$ in the gluon to be significantly greater than that of the sea quark to allow for the effects of the $g \to q\overline{q}$ convolution. In contrast, in the present calculation the effects of the $g \to q\overline{q}$ convolution are automatically included, by construction, and so the shadowing predictions should be more reliable than previous estimates. Actually, even the shadowing of the gluon distribution calculated dynamically turns out [4] to be smaller than that found in the parametrization adopted by KMRS [19] and MRS [3]. This explains the weaker shadowing corrections in the longitudinal structure function than that found in Refs. [19, 3].

Our perturbative QCD estimates may appear to be parameter-free and to give, in principle, "absolute" extrapolations of $F_2$ and $F_L$ into the small $x$ region. In practice there are significant ambiguities associated with the infrared (or nonperturbative) region. There is a dependence on the choice of cutoff $k_0^2$ in (21) used to calculate $f(z,k_T^2)$ and in the convolution formulas (17) and

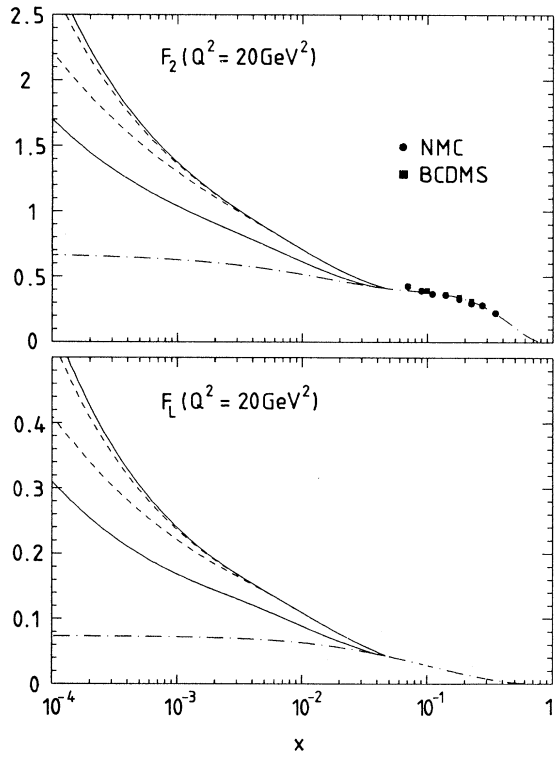


FIG. 6. As for Fig. 5 but for $Q^2 = 20$ GeV$^2$.

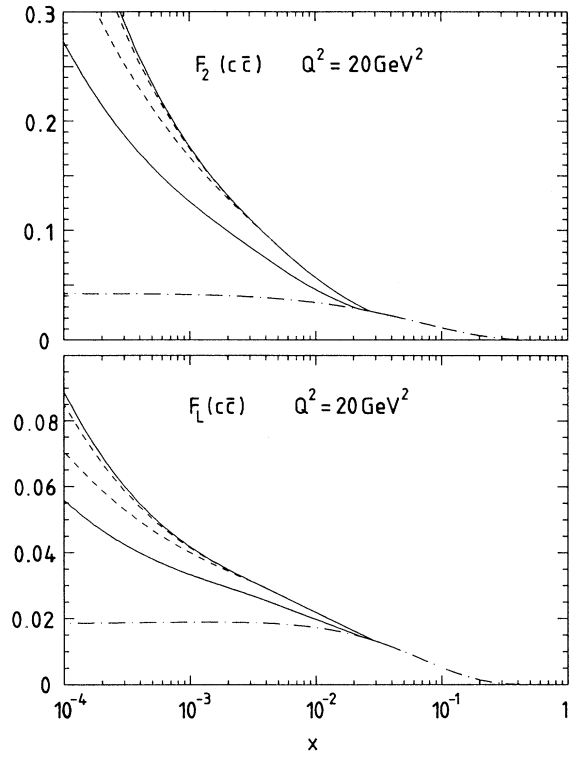


FIG. 7. As for Fig. 6 but showing only the $c\bar{c}$ contribution to $F_2(x, Q^2)$ at $Q^2 = 20$ GeV$^2$.

(18). For example, the lower continuous curves in Figs. 5 and 6 show the reduction in the estimates of $F_2$ and $F_L$ arising from increasing $k_0^2$ from 1 to 2 GeV$^2$. The reduction can be traced equally to (i) the change of effective slope and magnitude of the solution $f(z, k_T^2)$ of the Lipatov equation, and (ii) infrared effects in the convolution integrals (17) and (18).

Moreover, our estimates depend on contributions from low values of $\kappa_T'$ in (17) and (18). To quantify this dependence we introduce a nonzero mass $m_q$ for the light quarks. For example if we were to change $m_q$ from 0 to 1 GeV$^2$ our predictions for $F_2$ at $x \sim 10^{-3}$ would decrease by about 20%. This latter uncertainty is absent in the $c\bar{c}$ contribution, which we show separately in Fig. 7. Further discussion of heavy-quark production, which incorporates the small $x$ Lipatov effects can be found in Refs. [5–7, 20] (see also [21]).

## IV. DISCUSSION

In principle, the factorization formula (1) can give an absolute prediction of the deep-inelastic structure functions $F_i$ at small $x$, using the phenomenologically determined parton distributions at larger $x$, that is in the region $x > 0.01$ or so. The procedure we followed is to first solve the Lipatov equation to determine the (unintegrated) gluon distribution $f$ in the small $x$ region and then to convolute the result with exact gluon-virtual photon couplings $F_i^{(0)}$ as determined by the quark box diagrams. Symbolically, formula (1) may thus be written in the form

$$F_i = f \otimes F_i^{(0)}, \tag{24}$$

with $i = 2$ or $L$.

The above determination of the structure functions $F_i$ at small $x$ should be compared with the extrapolations based on the Altarelli-Parisi equations alone. The Altarelli-Parisi equations give the $\ln Q^2$ evolution of parton densities in terms of a set of "starting" distributions at some scale $Q_0^2 \gg \Lambda_{\rm QCD}^2$, chosen sufficiently high for perturbative QCD to be applicable. In this way the $x, Q^2$ behaviors of parton densities are given in terms of parametric forms at $Q^2 = Q_0^2$ with the parameters determined by fitting to the deep-inelastic structure function data. At present, however, the data do not extend into the small $x$ region (for $Q^2 \gg \Lambda_{\rm QCD}^2$), and the predictions for the structure functions at small $x$ are therefore entirely dependent on the particular parametric forms that are assumed for the $x \to 0$ behavior of the gluon and sea quark distributions. The parametric forms, although theoretically motivated, are to a large extent arbitrary. Consequently, extrapolations into the small $x$ domain from the region of the available data can, at best, just indicate general trends.

In contrast, the small $x$ behavior of the structure functions obtained via the factorization formula (24) results directly from QCD dynamics, at least in principle. Here the (unintegrated) gluon distribution $f$ is calculated at small $x$ by evolving the Lipatov equation in $\ln(1/x)$ from boundary conditions at $x = x_0 = 0.01$ which are specified by parton distributions determined from data at $x > x_0$. We therefore have, via (24), a theoretical prediction of the small $x$ behavior of the structure functions $F_{2,L}(x, Q^2)$ with the normalization determined by the data at larger $x$. In particular, we are able to make, for the first time, a quantitative prediction of the size of the shadowing corrections to $F_2$ and $F_L$. These corrections are found to be smaller than previous estimates and are almost certainly undetectable from structure function measurements at $x \sim 10^{-3}$.

Although the procedure to calculate $F_2$ and $F_L$ is well defined, in practice there are ambiguities (which, however, do not alter the conclusion concerning the relative size of the shadowing corrections). First we have the dependence on the lower cutoff $k_0^2$ required for the integration over the transverse momentum in the Lipatov equation (21) for $f(x, k_T^2)$. The exchanged gluons along the ladder are required to have transverse momenta of magnitude greater than $k_0$. The value of $\lambda$ in the effective $x^{-\lambda}$ behavior which emerges for $f$ at small $x$ is sensitive to the choice of $k_0^2$. Moreover, the same cutoff is necessary in the $k_T$ convolution integrals in (17) and (18). The $k_0^2$-dependent ambiguity is displayed in Figs. 5 and 6. The uncertainty is a reflection of uncalculable nonperturbative QCD effects.

A second ambiguity has its origin in the different $Q^2$ dependences which occur in the small and larger $x$ regions. It is well known [4] that the $Q^2$ dependence of the gluon distribution which emerges from the Lipatov equation is more rapid than that which results from the

Altarelli-Parisi equation. However, we have required the solution of the Lipatov equation to satisfy boundary conditions at $x = x_0 = 0.01$, which are obtained from the Altarelli-Parisi equation. Although the continuity of $f(x, Q^2)$ is ensured at $x = x_0$, the differing $Q^2$ dependences lead to artificial structure in the $x$ dependence just below the boundary, $x = x_0$. Only for a small region of $Q^2$ will smoothness across the boundary be obtained [4]. Fortunately, the region is $Q^2 = 10$–$20$ GeV$^2$, the region most pertinent to experiments at HERA. Since $F_2^g$ is a relatively small contribution at $x = 0.01$, the artificial structure would be barely noticeable in $F_2(x, Q^2)$ at the other values of $Q^2$. The main reason to draw attention to the deficiency is that it points to other contributions which could be important. The source of the problem is that the Lipatov equation is based on the leading $\ln(1/x)$ approximation, while to obtain a reliable $Q^2$ dependence it is necessary to include nonleading $\ln(1/x)$ contributions. Eventually it should be possible to overcome this problem by solving a more general evolution equation [22] for the gluon distribution which embodies both Lipatov effects and the complete Altarelli-Parisi equation.

In summary, we have formulated a procedure, based on perturbative QCD, which makes predictions of the structure functions $F_{2,L}(x, Q^2)$ for deep-inelastic electron-proton scattering in the small $x$ regime. In principle, the procedure overcomes the considerable uncertainties associated with the conventional parametric extrapolations to small $x$. In practice, we have seen it has its own ambiguities. The predicted values of the structure functions at $Q^2 = 10$ and $20$ GeV$^2$, including the effects of shadowing and displaying the theoretical uncertainties, are shown in Figs. 5–7.

## ACKNOWLEDGMENTS

We are grateful to Dick Roberts for providing us with parton distributions adapted from Ref. [3]. Three of us (J.K., A.J.A., and P.J.S.) thank the UK Science and Engineering Research Council for financial support. J.K. also thanks the Department of Physics and Grey College of the University of Durham for their warm hospitality.

[1] *Physics at HERA*, Proceedings of the Workshop, edited by W. Buchmüller and G. Ingelman (DESY, Hamburg, 1991).

[2] E.A. Kuraev, L.N. Lipatov, and V.S. Fadin, Zh. Eksp. Teor. Fiz. **72**, 712 (1977) [Sov. Phys. JETP **45**, 373 (1977)]; J.B. Bronzan and R.L. Sugar, Phys. Rev. D **17**, 585 (1978); Ya. Ya. Balitskij and L.N. Lipatov, Yad. Fiz. **28**, 1597 (1978)[Sov. J. Nucl. Phys. **28**, 822 (1978)]; L.N. Lipatov, Zh. Eksp. Teor. Fiz. **90**, 1536 (1986) [Sov. Phys. JETP **63**, 904 (1986)]; in *Perturbative QCD*, edited by A.H. Mueller (World Scientific, Singapore, 1989), p. 411; T. Jaroszewicz, Acta Phys. Pol. B **11**, 965 (1980); M. Ciafaloni, Nucl. Phys. **B296**, 49 (1988); S. Catani, F. Fiorani, and G. Marchesini, Phys. Lett. B **234**, 339 (1990); Nucl. Phys. **B336**, 18 (1990).

[3] A.D. Martin, R.G. Roberts, and W.J. Stirling, Phys. Rev. D **47**, 867 (1993).

[4] J. Kwiecinski, A.D. Martin, and P.J. Sutton, Phys. Lett. B **264**, 199 (1991); Phys. Rev. D **44**, 2640 (1991).

[5] S. Catani, M. Ciafaloni, and F. Hautman, Phys. Lett. B **242**, 91 (1990); Nucl. Phys. **B366**, 135 (1991).

[6] S. Catani, M. Ciafaloni, and F. Hautman, CERN Report No. CERN-TH-6398/92 (unpublished); S. Catani, CERN Report No. CERN-TH-6524/92 (unpublished).

[7] J.C. Collins and R.K. Ellis, Nucl. Phys. **B360**, 3 (1991).

[8] L.N. Gribov, E.M. Levin, and M.G. Ryskin, Phys. Rep. **100**, 1 (1983).

[9] J. Kwiecinski, A.D. Martin, and P.J. Sutton, Phys. Rev. D **46**, 921 (1992).

[10] M. Glück, R.M. Godbole, and E. Reya, Z. Phys. C **41**, 667 (1989); M. Glück, E. Reya, and A. Vogt, Z. Phys. C **48**, 475 (1990); **53**, 127 (1992); Dortmund University Report No. DO-TH-92-19 (unpublished).

[11] V. Barone *et al.*, University of Torino Report No. DFTT-8-92 (unpublished); Julich Report No. KFA-IKP-TH-1992-14 (unpublished).

[12] J.R. Forshaw, RAL report (in preparation).

[13] L.N. Lipatov and G.V. Frolov, Yad. Fiz. **13**, 588 (1971) [Sov. J. Nucl. Phys. **13**, 333 (1971)].

[14] J. Bartels, M. Loewe, and A. de Roeck, Z. Phys. C **54**, 635 (1992).

[15] E.M. Levin and M.G. Ryskin, Yad. Fiz. **53**, 1052 (1991) [Sov. J. Nucl. Phys. **53**, 653 (1991)].

[16] R.G. Roberts (private communication).

[17] New Muon Collaboration, P. Amaudruz *et al.*, Phys. Lett. B **295**, 159 (1992).

[18] BCDMS Collaboration, A.C. Benvenuti *et al.*, Phys. Lett. B **223**, 485 (1989).

[19] J. Kwiecinski, A.D. Martin, R.G. Roberts, and W.J. Stirling, Phys. Rev. D **42**, 3645 (1990).

[20] B.R. Webber, in *QCD at 200 TeV*, Proceedings of the 17th Workshop, Erice, Italy, 1990, edited by L. Cifarelli and Y. Dokshitzer (Plenum, New York, 1992); B.R. Webber, *Physics at HERA* [1], Vol. 1, p. 285; G. Marchesini and B.R. Webber, Nucl. Phys. **B386**, 215 (1992).

[21] E.M. Levin, M.G. Ryskin, V.T. Kim, Yu.M. Shabelski, and A.G. Shuvaev, Yad. Fiz. **54**, 1420 (1991) [Sov. J. Nucl. Phys. **54**, 867 (1991)].

[22] G. Marchesini, in *QCD at 200 TeV* [20].